Dinuclear Chromium(V) Amino Acid Complexes from the Reduction of Chromium(VI) in the Presence of Amino Acid Ligands: XAFS Characterization of a Chromium(V) Amino Acid Complex

Henrietta A. Headlam, Colin L. Weeks, Peter Turner, Trevor W. Hambley, and Peter A. Lay*

Centre for Heavy Metals Research, School of Chemistry, University of Sydney, NSW 2006, Australia

Received April 6, 2001

The first synthesis and characterization of Cr(V) complexes of non-sulfur-containing amino acids are reported. The reduction of Cr(VI) in methanol in the presence of amino acids glycine, alanine, and 2-amino-2-methylpropanoic acid (α-aminoisobutyric acid, Aib) yielded several Cr(V) EPR signals. For the reaction involving glycine, the only Cr(V) EPR signals detected were those of the Cr(V)−intermediate methanol complexes, which were also observed in the absence of amino acids. The reaction involving alanine yielded one Cr(V) signal with a g_{iso} value of 1.9754 ($a_{iso} = 4.88 \times 10^{-4}$ cm^{-1} and $A_{iso}(^{53}Cr) = 17.89 \times 10^{-4}$ cm^{-1}). However, a solid product isolated from the reaction solution was EPR silent and was characterized as a dioxo-bridged dimeric species, $[Cr^{V}_2(\mu\text{-}O)_2(O)_2(Ala)_2(OCH_3)_2]^{2-}$, by multiple-scattering XAFS analysis and electrospray mass spectrometry. The EPR spectrum of the reduction reaction of Cr(VI) in the presence of Aib showed several different Cr(V) signals. Those observed at lower g_{iso} values (1.9765, 1.9806) were assigned to Cr(V)−methanol intermediates, while the relatively broad six-line signal at $g_{iso} = 2.0058$ was assigned as being due to a Cr(V) complex with coupling to a single deprotonated amine group of the amino acid. This was confirmed by simplification of the superhyperfine coupling lines from six to three when the deuterated ligand was substituted in the reaction. The reduction of Cr(VI) with excess alanine or Aib ligands resulted in the formation of tris-chelate Cr(III) complexes, which were analytically identical to complexes formed via Cr(III) synthesis methods. The *fac*-$[Cr(Aib)_3]$ complex was characterized by single-crystal X-ray diffraction.

Introduction

The reduction of Cr(VI) by the thiol group of glutathione (γ-Glu-Cys-Gly, GSH) produces Cr(VI), Cr(V), Cr(IV), and Cr(III) thiol esters, which are postulated to be involved in Cr(VI) genotoxicity.[1] Kinetic studies have used *L*-Cys as a model for GSH.[2−7] Cr(VI) is reduced more rapidly by *L*-Cys than GSH (pH 7.0−7.6)[8] and *L*-Cys reacts with Cr(VI) via both the thiolate and amine groups.[7] A second *L*-Cys coordinates to form a Cr(V) complex, which is assigned as **I** (or an isomer).[7] Subsequently, **I** undergoes rapid reduction to a complex, which has the previously free carboxylates bound to Cr(III).[7] The Cr(V)−cysteine EPR signals are pH dependent (pH 3−7) with g_{iso} values varying from 1.984 to 1.987, line widths from 8.1 to 18.2 G, and a decrease in signal intensity with an increase in pH value; no signal is observed at pH ≥ 8.0.[9] During the reduction of Cr(VI) with GSH, two Cr(V) EPR signals with g_{iso} values of 1.996 and 1.986 were observed with a similar pH dependence as the Cr(V)−cys EPR signals. At pH ≤ 4, the two signals were replaced by a third at $g_{iso} \sim 1.990$.[9] The intensity of the Cr(V) EPR signal at g_{iso} 1.996 increased as the GSH/Cr(VI) ratio was increased,[9,10] but the $g_{iso} = 1.986$ signal was saturated at low [GSH].[9]

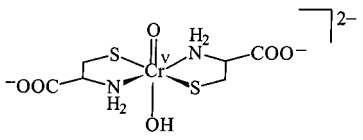

I

The question remains whether non-sulfur-containing peptide and amino acid complexes are among the species generated in vivo. Long-lived Cr(V) complexes of non-sulfur containing peptides were produced during the Cr(VI)/MeOH reaction in the presence of glycine and alanine peptides.[11] Unlike GSH, these peptides did not reduce Cr(VI) at any significant rate.[11,12] Hence, MeOH was required in the reactions to reduce Cr(VI) to Cr(V) and the reaction required light to initiate and/or increase the reaction rate; Cr(VI)−peptide reactions performed in the dark yielded only very weak EPR signals.[11,12] Chromium(V)−peptide complexes were also generated by oxidation of Cr(III)

(1) O'Brien, P.; Kortenkamp, A. *Transition Met. Chem.* **1995**, *20*, 636−642.
(2) Kwong, D. W. J.; Pennington, D. E. *Inorg. Chem.* **1984**, *23*, 2528−2532.
(3) Connett, P. H.; Wetterhahn, K. E. *J. Am. Chem. Soc.* **1985**, *107*, 4282−4288.
(4) O'Brien, P.; Pratt, J.; Swanson, F. J.; Thornton, P.; Wang, G. *Inorg. Chim. Acta* **1990**, *169*, 265−269.
(5) Brauer, S. L.; Wetterhahn, K. E. *J. Am. Chem. Soc.* **1991**, *113*, 3001−3007.
(6) O'Brien, P.; Wang, G.; Wyatt, P. B. *Polyhedron* **1992**, *11*, 3211−3216.
(7) Levina, A.; Lay, P. A. *Inorg. Chem.* **1996**, *35*, 7709−7717.
(8) Standeven, A. M.; Wetterhahn, K. E. *Chem. Res. Toxicol.* **1991**, *4*, 616−625.
(9) Kitagawa, S.; Seki, H.; Kametani, F.; Sakurai, H. *Inorg. Chim. Acta* **1988**, *152*, 251−255.
(10) Goodgame, D. M. L.; Joy, A. M. *J. Inorg. Biochem.* **1986**, *26*, 219−224.
(11) Headlam, H. A.; Lay, P. A. *Inorg. Chem.* **2001**, *40*, 78−86.
(12) Headlam, H. A., Ph.D. Thesis, University of Sydney, 1999.

10.1021/ic010377l CCC: $20.00
Published on Web 08/24/2001

analogues and showed a pH dependence of the Cr(V) EPR speciation.[12,13] At low pH values (~4), signals due to monomeric six-coordinate complexes were observed with g_{iso} values between 1.9822 and 1.9844.[13] At pH values ≥ 5.6, the intensities of the aforementioned signals decreased and a second broader signal appeared at $g_{iso} \approx 1.966$.[13] In the present study, the formation of Cr(V)−amino acid complexes was studied using UV−vis and EPR spectroscopy from the oxidation of Cr(III) and reduction of Cr(VI), and a dinuclear alanine complex was isolated and characterized by ESMS and XAFS.

Experimental Section

Glycine (Sigma, 98%), alanine (Merck, 98%) and 2-amino-2-methylpropanoic acid (α-aminoisobutyric acid, Aib; Sigma, 99%) were used without further purification. Other reagents included $CrCl_3 \cdot 6H_2O$ (Merck, 98%), $Na_2Cr_2O_7 \cdot 2H_2O$ (Merck, 98%), NaOH (Merck, 98%), HIO_4 (Hopkins and Williams, 95%), PbO_2 (Merck, AR grade), BN (Fluka, AR grade), MeOH (Biolab Scientific, AR grade), and CH_3OD (Sigma, 99.9%) were used as received. Water was distilled and/or deionized.

Caution: *Cr(VI) is carcinogenic and mutagenic*[14] *and Cr(V) complexes are mutagenic and potential carcinogens.*[15−17] *Appropriate precautions should be taken to avoid inhalation of Cr(VI) and skin contact while handling solutions of these chemicals.*

Physical Measurements. Electronic absorption spectra were recorded on a Hewlett-Packard 8452A diode-array spectrophotometer (190−820 nm) using a 1-cm quartz cell. IR spectra were recorded with a Bio Rad FTS-40 spectrophotometer from ~15% w/w KBr (Sigma, IR grade) mulls. Electrospray mass spectra were obtained using a Finnigan LCQ ESI-APCI Triple quadrupole mass spectrometer; operating conditions: ESI spray voltage, 5 kV; nitrogen sheath gas pressure, 60 psi; capillary temperature, 200 °C. For loop injection, the mobile phase was 50% v/v aqueous MeOH with 1% v/v acetic acid, and the flow rate was 100 μL min^{-1}. Microanalyses were performed by the Australian National University Microanalytical Service.

EPR spectra were recorded using a quartz flat cell and a Bruker EMX EPR spectrometer with a Hewlett-Packard ER 085C Magnet and an ER0 41XG Microwave Bridge (X-band, ~9.6 GHz). The spectra were calibrated using a Bruker EMX Microwave Bridge Controller and an EMX 032T Field Controller. Operating parameters were: microwave power, 200 mW; modulation frequency, 100 kHz; modulation amplitude, 2.07, 1.07 or 0.57 G; receiver gain, 1×10^5 or 2×10^4; conversion time, 20.48 ms; time constant, 5.12 ms; sweep time, 20.972 s; temperature, ~20 °C; and number of scans, 5. Second-order corrections were applied to A_{iso} values.

Synthesis of Cr(III) Amino Acid Complexes. The Cr(III) complexes of Aib and Ala were prepared according to the literature method for the glycine complex.[18]

***fac*-[$Cr^{III}(Aib)_3$].** A MeOH solution (100 mL) of $CrCl_3 \cdot 6H_2O$ (2.00 g, 7.5 mmol) and Aib (4.75 g, 45 mmol) was refluxed for 12 h until the solution turned deep red. After filtration of unreacted ligand, a solution of NaOH (1.66 g, 40 mmol) in MeOH (40 mL) was added dropwise with stirring. A crop of bright pink crystals grew over several days and these were collected at the pump and dried for 24 h in a desiccator. Yield: 0.06 g (~2%). Anal. Calcd for $[Cr(C_4H_8NO_2)_3]0.4NaOCH_3$: C, 39.19; H, 6.69; N, 11.06. Found: C, 39.22; H, 6.79; N, 10.96. ES/MS (aq MeOH, +ve ion): 359 (20%) and 381 (100%) *m*/*z*. UV−vis (water): 388 (93 M^{-1} cm^{-1}) and 512 (120 M^{-1} cm^{-1}). IR (KBr mull): 3240/3222 w, 3146 m, 2967 w, 1664 s, 1608 m, 1563 w, 1475 w, 1387 m, 1365 w, 1328 m, 1224 m, 1195 w, 1148 w, 1128 w, 1099 w, 966 w, 893 w, 824 w, 783 w, 701 w, 659 w, 638 w, 574 w, 567 w, 529 w, 413 w cm^{-1}.

[$Cr^{III}(Aib)_3$]. Attempts to repeat the synthesis of the pure *fac* isomer resulted in a mixture of *fac* and *mer* isomers as a crimson red solid in a higher yield: 0.83 g (28%). Anal. Calcd for $[Cr(C_4H_8NO_2)_3]0.5H_2O$: C, 39.21; H, 5.93; N, 10.99. Found: C, 39.26; H, 5.89; N, 10.87. UV−vis (water): 382 (128 M^{-1} cm^{-1}) and 520 (124 M^{-1} cm^{-1}). IR (KBr mull): 3290 w, 3237 w, 3200 w, 3080 w, 3003 w, 2987 w, 2935 w, 2877 w, 2359 w, 1663 m, 1637 s, 1625 s, 1594 w, 1569 m, 1473 w, 1388 m, 1348 m, 1232 w, 1198 w, 1148 w, 1125 w, 1115 w, 1098 w, 1013 w, 966 w, 899 w, 826 w, 779 w, 725 w, 640 w, 578 w, 564 w, 518 w, 422 m cm^{-1}.

[$Cr^{III}(Ala)_3$]. Yield of pink solid: 0.95 g (~54%). Anal. Calcd for $[Cr(C_3H_6NO_2)_3] \cdot 0.5H_2O$: C, 33.23; H, 5.89; N, 12.92. Found: C, 33.24; H, 6.54; N, 12.93. ES/MS (aq MeOH, +ve ion): 319 (41%) and 339 (100%) *m*/*z*. UV−vis (water): 380 (74 M^{-1} cm^{-1}) and 514 (76 M^{-1} cm^{-1}). IR (KBr mull): 3313 w, 3240/3218 m, 3137 m, 2987 w, 2937 w, 1699 m, 1662 s, 1631 s, 1600 m, 1559 w, 1457 w, 1412 w, 1386 w, 1374 w, 1353 m, 1235 w, 1203 w, 1184 w, 1151 w, 1113 w, 1068 w, 1023 w, 923 w, 859 m, 776 w, 742 w, 706 w, 694 w, 647 w, 623 w, 560 m, 526 w, 418 w cm^{-1}.

Oxidation Reactions. [$Cr^{III}(Aib)_3$] was oxidized using either HIO_4 or PbO_2. A solution of [$Cr^{III}(Aib)_3$] (4.5 mg, ~4 mM) in water (3.0 mL) was prepared and a zero-time UV−vis spectrum was recorded. To the solution was added HIO_4 (5.2 mg) and UV−vis spectra were recorded at 1, 5, 10, 20, 40, 50, 60, 80, 100, and 120 min after mixing. PbO_2 oxidations were studied at 37 °C on ~5 mM solutions of [$Cr^{III}(Aib)_3$] (18.9 mg in 10.0 mL water). A 1-mL aliquot was removed and the zero-time spectrum was recorded. The solution was then placed into a water bath (37 °C) and allowed to equilibrate before adding PbO_2 (58.9 mg). After PbO_2 was added, 1-mL aliquots of the reaction solution were removed at 1, 5, 10, 20, 30, 40, 50, and 60 min and were centrifuged to remove solid unreacted PbO_2. The UV−vis spectra of the resultant supernatants were recorded. The oxidation reactions were repeated at a concentration of 50 mM with a four-molar excess of PbO_2 for recording EPR spectra.

Reduction Reactions. For reactions in MeOH (100.0 mL), $Na_2Cr_2O_7 \cdot 2H_2O$ (1.49 g, 50 mM) was dissolved and 15.0-mL aliquots were added to three pairs of glass vials into which the finely ground glycine (0.23 g), alanine (0.27 g), or Aib (0.31 g) had been preweighed to give 200 mM solutions. One set of vials was wrapped in foil for dark reactions, while the second was exposed to light from a fluorescent lamp (distance ~20 cm, Norax brand, 18" × 1" 15-W tube). Reactions in water as the solvent were performed as described for the MeOH reactions. Redox reactions were also performed with excess ligand (>600 mM) in both the presence and absence of light. EPR spectra of the reaction solutions were recorded at appropriate time intervals depending on the overall rate of the reaction. Finally, an experiment was conducted using an Aib ligand that was deuterated on the amine group by dissolving the ligand in D_2O, removing excess ligand by filtration, and isolating the deuterated ligand by rotary evaporation (~80 °C). The reduction of Cr(VI) (50 mM) was performed in CH_3OD with *N*-deuterated Aib (200 mM) in the light and EPR spectra were recorded at 3-d intervals.

Synthesis of Cr(V) Amino Acid Complexes. For each Cr(V)/amino acid complex, optimum conditions for its preparation from the reduction of Cr(VI) in MeOH were determined from the EPR and UV−vis spectroscopic experiments.

Cr(V)−Glycine Complex. $Na_2Cr_2O_7 \cdot 2H_2O$ (0.24 g) and glycine (0.26 g) in MeOH (16 mL) were reacted in the presence of fluorescent light for ≥ 30 d. After such time, the fine brown precipitate was collected by filtration through a sintered glass funnel. Yield: 0.19 g (61.2%). Anal. Calcd for $Na_2[Cr_2O_4(C_2H_4NO_2)_2(OCH_3)_2] \cdot 1.2C_2H_5NO_2$: C, 19.62; H, 3.92; N, 8.72. Found: C, 19.89; H, 3.75; N, 8.78. ES/MS (aq MeOH, +ve ion): 297, 413, 457 and 494 *m*/*z*. UV−vis (water): 380 nm (1345 M^{-1} cm^{-1}). IR (KBr mull): 3245 m, br, 2943 w, 2826 w, 1653 s, 1559 m, 1374 m, 1326 m, 1136 w, 1042 m, 920 w, 805 w, 748 w, 537 s, 472 m, 458 m cm^{-1}.

(13) Headlam, H. A.; Lay, P. A. To be submitted.
(14) IARC *Monographs of the Evaluation of the Carcinogenic Risk of Chemicals to Humans*; International Agency for Research on Cancer: Lyon, France, 1990.
(15) Farrell, R. P.; Judd, R. J.; Lay, P. A.; Dixon, N. E.; Baker, R. S. U.; Bonin, A. M. *Chem. Res. Toxicol.* **1989**, *2*, 227−229.
(16) Dillon, C. T.; Lay, P. A.; Bonin, A. M.; Dixon, N. E.; Collins, T. J.; Kostka, K. L. *Carcinogenesis* **1993**, *14*, 1875−1880.
(17) Levina, A.; Barr-David, G.; Codd, R.; Lay, P. A.; Dixon, N. E.; Hammershøi, A.; Hendry, P. *Chem. Res. Toxicol.* **1999**, *12*, 371−381.
(18) Bryan, R. F.; Greene, P. T.; Stokely, P. F.; Wilson Jr., E. W. *Inorg. Chem.* **1971**, *10*, 1468−1473.

Cr(V)−Alanine Complex. $Na_2Cr_2O_7 \cdot 2H_2O$ (1.78 g) and alanine (2.13 g) were reacted in MeOH (50 mL) in the dark for 5 d at room temperature. After such time, the solution turned dark brown and excess ligand was removed by filtration. The filtrate was rotary evaporated to remove MeOH and the resulting dark brown solid was stored in a desiccator. Yield: 1.15 g (43.7%). Anal. Calcd for $Na_2[Cr_2O_4(C_3H_6NO_2)_2(OCH_3)_2]0 \cdot 5(C_3H_7NO_2).0 \cdot 5CH_3OH$: C, 23.42; H, 4.62; N, 6.83; Cr, 19.7; Na 8.7. Found: C, 23.79; H, 4.46; N, 6.92; Cr 20.7; Na, 7.9. ES/MS (aq MeOH, +ve ion): 206, 356, 450 and 561 *m*/*z*. UV−vis (water): 374 nm (1475 M^{-1} cm^{-1}). IR (KBr mull): 3939 w, 3232 m, br, 2985 w, 1653 s, 1559 m, 1457 m, 1387 m, 1362 w, 1288 w, 1113 m, 1057 w, 909 m, 865 m, 786 m, 614 w, 559 w, 526 w, 516 w, 418 w cm^{-1}.

XAS Data Collection. The K-edge X-ray absorption spectrum of $Na_2[Cr^V_2O_4(Ala)_2(OCH_3)_2].0 \cdot 5(AlaH).0 \cdot 5CH_3OH$ was collected at the Australian National Beamline Facility, beamline 20B at the KEK Photon Factory in Tsukuba, Japan. The ring energy was 2.5 GeV and the ring current was 200−400 mA. The Si channel-cut 111 crystal monochromator was detuned 50% to reduce harmonic contamination. A finely ground mixture of $Na_2[Cr^V_2O_4(Ala)_2(OCH_3)_2].0 \cdot 5(AlaH).0 \cdot 5CH_3OH$ (22.6 mg) and BN (30.7 mg) was placed in a 0.5-mm-thick Al holder sealed with Kapton tape on both sides. A constant sample temperature of 14 K was maintained by a Cryo Industries liquid helium cryostat (model number REF-1577-D22), controlled by a Neocera LTC-11 temperature controller. Transmission spectra were collected using ionization chambers filled with nitrogen gas. Three scans were recorded (5770−7050 eV); the position of the beam was moved to a fresh area of the sample for each scan to minimize the effects of any photoinduced sample decomposition. The energy was calibrated against a 16% Cr in stainless steel foil, assigning the strongest inflection point at the edge to an energy of 6005.0 eV.[21]

XAFS Data Analysis. XAS were averaged and monochromator glitches were removed. A second-order polynomial was fitted to the pre-edge region, extrapolated into the XAFS region, and subtracted to remove the underlying absorbance. A three-region spline polynomial was fitted to the XAFS region and then subtracted. The data (normalized to an edge jump of 1.0) were converted to *k* space, where *k* is the photoelectron wavevector $k = \hbar^{-1}\sqrt{2m_e(E-E_0)}$, m_e is the electron mass, E_0 is the threshold energy for the 1s→continuum transition, *E* is the energy of the absorbed X-ray photon, and $(E - E_0)$ is the energy of the generated photoelectron. Data were multiplied by k^3 to compensate for decreasing XAFS intensity with increasing photoelectron energy.

Model-fitting calculations were performed using XFIT.[19−21] This program incorporates ab initio calculations of the XAFS using the programs FEFF 4.06[22,23] for single-scattering (SS) and FEFF 6.01[24,25] for multiple-scattering (MS) analyses. The model structures were refined to optimize the fit of the calculated to the observed XAFS. The parameters varied in the refinements were as follows: the *x*, *y*, *z* coordinates for each atom in the model, the Debye−Waller factor, σ^2, of every atom in the model (except the absorbing atom), a scale factor S_0^2, and E_0. Restraints on S_0^2, the Debye−Waller factors, bond lengths and some bond angles were included in the refinements; the restraints on the bond lengths and angles of the alanine ligand were obtained from the crystal structure of $[Cr^{III}_2(OH)_2(Ala)_4]$.[26] In the MS analysis, the plane-wave and curved-wave path filter thresholds were set at 2% and 3% of the strongest SS path, respectively. In the dinuclear models, one of the Cr atoms was defined as the absorber and the second was treated only as a backscatterer. Symmetry constraints were used in the dinuclear models to reduce the number of parameters refined so that the refinements were overdetermined.[27] The *x*, *y*, and *z* coordinates of atoms in the half of the molecule containing the "backscattering" Cr atom were constrained to be equivalent to the coordinates of the atoms about the "absorbing" Cr atom. The goodness of fit parameter, *R*, was calculated by the method of Ellis and Freeman.[20] Errors in bond lengths and some bond angles due to the noise in the XAFS data were estimated by the Monte Carlo method included in the XFIT program.[19,20] These were combined with conservative systematic errors[28−30] to produce the probable errors in bond lengths and angles.[31]

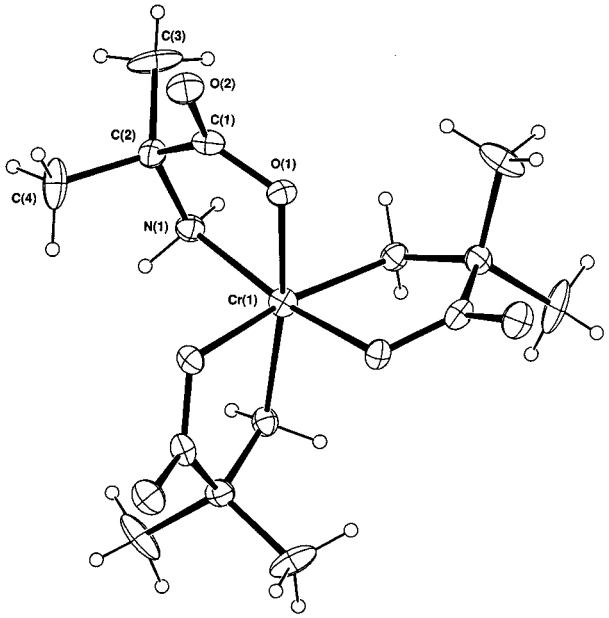

Figure 1. An ORTEP depiction of the *fac*-$[Cr(NH_2C(CH_3)_2CO_2)_3]$ complex, with 20% atom displacement ellipsoids.

X-ray Crystallography. A pink acicular 0.20 × 0.02 × 0.02 mm crystal of *fac*-$[Cr(Aib)_3]$ was attached to a thin glass fiber and mounted on a Rigaku AFC7R diffractometer employing graphite monochromated CuKα radiation generated from a rotating anode. Cell constants were obtained from a least-squares refinement against 25 reflections located between 18.20 and 49.40° 2θ. Data were collected at 294(2) K with ω:2θ scans to 119.82° 2θ. The intensities of three standard reflections measured every 150 reflections decreased by 4.95% during the data collection and a correction was accordingly applied to the data. The crystal faces were indexed and an analytical absorption correction was applied to the data.

Processing and calculations were undertaken with TEXSAN.[32] The structure was solved in the space group *R*3*c* (#161) by direct methods with SHELXS-86,[33] and extended and refined with SHELXL-97[34] using the TEXSAN interface.[32] Although not unambiguous, the reflection statistics appeared to be acentric, and a satisfactory solution was not obtained in the centrosymmetric space group $R\bar{3}c$(#167). The *R*3*c* asymmetric unit contains one-third of a complex molecule, with the

(19) Ellis, P. J., Ph.D. Thesis, The University of Sydney, 1995.
(20) Ellis, P. J.; Freeman, H. C. *J. Synchrotron Rad.* **1995**, *2*, 190−195.
(21) Ellis, P. J. *XFIT for Windows 95*; Australian Synchrotron Research Program: Sydney, 1996.
(22) de Leon, J. M.; Rehr, J. J.; Zabinsky, S. I.; Albers, R. C. *Phys. Rev. B* **1991**, *44*, 4146−4156.
(23) Rehr, J. J.; de Leon, J. M.; Labinsky, S. I.; Albers, R. C. *J. Am. Chem. Soc.* **1991**, *113*, 5135−5140.
(24) Rehr, J. J.; Albers, R. C.; Zabinsky, S. I. *Phys. Rev. Lett.* **1992**, *69*, 3397−3400.
(25) Zabinsky, S. I.; Rehr, J. J.; Ankudinov, A.; Albers, R. C.; Eller, M. J. *Phys. Rev. B* **1995**, *52*, 2995−3009.
(26) Ranger, G.; Beauchamp, A. L. *Acta Crystallogr., Sect. B* **1981**, *B37*, 1063−1067.
(27) Binsted, N.; Strange, R. W.; Hasnain, S. S. *Biochemistry* **1992**, *31*, 12117−12123.
(28) Gurman, S. J. *J. Synchrotron Rad.* **1995**, *2*, 56−63.
(29) Riggs-Gelasco, P.; Stemmler, T. L.; Penner-Hahn, J. E. *Coord. Chem. Rev.* **1995**, *144*, 245−286.
(30) Garner, C. D. *Adv. Inorg. Chem.* **1991**, *36*, 303−339.
(31) Rich, A. M.; Armstrong, R. S.; Ellis, P. J.; Freeman, H. C.; Lay, P. A. *Inorg. Chem.* **1998**, *37*, 5743−5753.
(32) *TEXSAN: Crystal Structure Analysis Package*; Molecular Structure Corporation, 1985 and 1992.
(33) Sheldrick, G. M. In *Crystallographic Computing 3*; Sheldrick, G. M., Kruger C., Goddard, R., Eds.; Oxford University Press: New York, 1985; pp 175−189.
(34) Sheldrick, G. M. *SHELXL97, Program for crystal structure refinement*; University of Göttingen: Germany, 1997.

Table 1. Crystallographic Data for *fac*-[$Cr^{III}(Aib)_3$] Complex

formula of the refinement model	$C_{12}H_{24}CrN_3O_6$
model molecular weight	358.34
crystal system	trigonal
space group	*R*3*c*(#161)
a	17.301(8) Å
c	9.686(7) Å
V	2511(2) Å^3
D_c	1.422 g cm^{-3}
Z	6
μ (Cu Kα)	5.911 mm^{-1}
T (analytical)$_{min,max}$	0.742, 0.886
$2\theta_{max}$	119.82°
hkl range	−16 16, 0 19, 0 10
N	937
N_{ind}	447(R_{merge} 0.145)
N_{obs}	221($I > 2\sigma(I)$)
N_{var}	69
residuals[a] R1(*F*), wR2(F^2)	0.0365, 0.0931
GoF (all)	0.927
residual extrema	−0.369, 0.338 e Å^{-3}

[a] $R1 = \sum||F_0| - |F_c||/\sum|F_0|$ for $F_0 > 2\sigma(F_0)$; $wR2 = (\sum w(F_0^2 - F_c^2)^2/\sum(wF_c^2)^2)^{1/2}$ all reflections; $w = 1/[\sigma^2(F_0^2) + (0.0202P)^2]$ where $P = (F_0^2 + 2F_c^2)/3$.

Table 2. Selected Bond Lengths and Angles for the *fac*-isomers of the Cr(III) Complexes of Aib and Gly[18]

	[$Cr^{III}(Aib)_3$]	[$Cr^{III}(Gly)_3$][18]
bond lengths (Å)		
Cr−N	2.067(9)	2.068(5)
Cr−O	1.939(7)	1.965(2)
N−C	1.471(12)	1.479(3)
C1−C2	1.540(14)	1.517(2)
O1−C1	1.327(12)	1.290(9)
O2−C1	1.241(11)	1.223(6)
bond angles (deg)		
N−Cr−O (intra ligand)	81.7(3)	81.7(1)
O−Cr−O	90.6(4)	92.8(1)
N−Cr−N	95.0(4)	95.9(1)
O−Cr−N (long)	171.4(4)	174.1(1)
O−Cr−N (short)	93.2(4)	89.7(1)

metal located on a 3-fold axis. Anisotropic thermal parameters were refined for the non-hydrogen model atoms and a riding atom model was used for the hydrogen atoms. An ORTEP[35] depiction of the molecule is provided in Figure 1. The absolute structure was established with the Flack parameter[36] refining to 0.06(4). Crystallographic data and selected bond distances and bond angles are listed in Tables 1 and 2, respectively. Complete crystallographic details are included in the Supporting Information (Tables S1−S9).

Bond Valence Sum Calculations. The bond valence sum (BVS) of the Cr in the Cr(V)−alanine complex was calculated using eq 1:[37]

$$\mathrm{BVS} = \sum_j S_{ij} \tag{1}$$

where

$$s_{ij} = \exp\{(R_0 - R_{ij})/0.37] \tag{2}$$

where R_0 is a bond length of unit valence and R_{ij} is the observed bond length. The value of R_0 depends on the nature of the atoms *i* and *j*. An average value of $R_0 = 1.724$ Å was used for the Cr−O bonds.[37] There has been no report of a value of R_0 for Cr−N bonds in the literature, so an average value of $R_0 = 1.83$ Å (s.d. = 0.06 Å), was estimated from the crystal structures of 15 Cr(III) and Cr(V) complexes that contained either N or mixed N/O donor ligands.[26,38] The complexes contained a range of N donor groups: nitrido, amido, imine, amine, imidazole, and porphyrin.

Results

Crystal Structure of *fac*-[$Cr^{III}(Aib)_3$]. The structure of the *fac*-isomer is similar to that of [$Cr^{III}(Gly)_3$][18] (Figure 1, Table 2). The Cr(1)−N(1) and C(1)−C(2) bond lengths are 2.067(9) Å and 1.540(14) in the [$Cr^{III}(Aib)_3$] complex, and 2.068(5) Å and 1.517(2) Å in the [$Cr^{III}(Gly)_3$] complex. The metal ion is located on a 3-fold axis and the ligand plane forms an angle of 61.2(4)° with this axis. The metal is 0.51(2) Å from the ligand O(1)−N(1)−C(1)−C(2) least-squares plane.

Oxidation Reactions of [$Cr^{III}(Aib)_3$]. The λ_{max} values obtained from the electronic absorption spectra of the Cr(III) amino acid complexes are summarized in the Supporting Information (Table S10). Oxidation of [$Cr^{III}(Aib)_3$] was studied using both UV−vis and EPR spectroscopies. When periodic acid was used as the oxidant (Figure 2a), a shift in the λ_{max} value from 388 to 374 nm occurred within 10 min and was accompanied by a color change from pink to brown. After further oxidation, the reaction turned yellow, the λ_{max} value shifted to 352 nm, and the absorbance increased to produce a typical Cr(VI) spectrum. No EPR signals were observed over similar time intervals in a duplicate oxidation reaction. For PbO_2 oxidations (Figure 2b), the UV−vis spectra were slightly different to those generated during the HIO_4 oxidations. After 10 min, the λ_{max} value shifted from 388 to 378 nm, with a concomitant color change from pink to brown. As the oxidation period increased, the absorption at 378 nm also increased and the solution changed color to yellow, showing again that Cr(VI) was the end product. No Cr(V) signals were observed in the EPR spectra.

Reduction of Cr(VI) in the Presence of Amino Acids. In water, there was no discernible reduction of Cr(VI) in the presence of glycine, alanine, or Aib for both the light and dark reactions, even after several months. However, when the reactions were performed in MeOH, the solutions turned brown and several Cr(V) signals were detected by X-band EPR spectroscopy. The control Cr(VI)/MeOH reaction yielded two Cr(V) EPR signals with g_{iso} values of 1.9765 and 1.9687.[11,12] The reduction of Cr(VI) by MeOH in the presence of glycine resulted in similar Cr(V) signals with g_{iso} values of 1.9765 and 1.9697. When reacted in light, the intensity of the first signal increased from the start of the reaction and reached a maximum value at day 15 (Figure 3a). After such time, its intensity decreased until it had almost disappeared by the end of four weeks. The second signal did not appear to change with time until after 20 d of the reaction had passed, after which time its intensity decreased. At the end of the reaction, the fine brown precipitate that formed was collected and analyzed. Neither the brown solid, nor its aqueous solution, gave Cr(V) EPR signals.

(35) (a) Johnson, C. K. *ORTEPII*, Report ORNL-5138; Oak Ridge National Laboratory: Oak Ridge, TN, 1976. (b) *Xtal3.6 System*; Hall, S. R., du Boulay, D. J., Olthof-Hazekamp, R., Eds.; University of Western Australia: Australia, 1999.

(36) (a) Flack, H. D. *Acta Crystallogr., Sect A* **1983**, *39A*, 876−881. (b) Bernardinelli, G.; Flack, H. D. *Acta Crystallogr., Sect A* **1985**, *41A*, 500−511.

(37) Wood, R. M.; Abboud, K. A.; Palenik, R. C.; Palenik, G. J. *Inorg. Chem.* **2000**, *39*, 2065−2068.

(38) Srinivasan, K.; Kochi, J. K. *Inorg. Chem.* **1985**, *24*, 4671−4679. Che, C.-M.; Ma, J.-X.; Wong, W.-T.; Lai, T.-F.; Poon, C.-K. *Inorg. Chem.* **1988**, *27*, 2547−2548. Collins, T. J.; Slebodnick, C.; Uffelman, E. S. *Inorg. Chem.* **1990**, *29*, 3433−3436. Murdoch, C. M.; Cooper, M. K.; Hambley, T. W.; Hunter, W. N.; Freeman, H. C. *J. Chem. Soc., Chem. Commun.* **1986**, 1329−1331. Azuma, N.; Imori, Y.; Yoshida, H.; Tajima, K.; Li, Y.; Yamauchi, J. *Inorg. Chim. Acta* **1997**, *266*, 29−36. Choi, J.-H.; Suh, I.-H.; Kwak, S.-H. *Acta Crystallogr. Sect. C* **1995**, *C51*, 1745−1748. Groves, J. T.; Takahashi, T.; Butler, W. M. *Inorg. Chem.* **1983**, *27*, 884−887. Collins, T. J.; Santarsiero, B. D.; Spies, G. H. *J. Chem. Soc., Chem. Commun.* **1983**, 681−682. Oki, H.; Yoneda, H. *Inorg. Chem.* **1981**, *20*, 3875−3879.

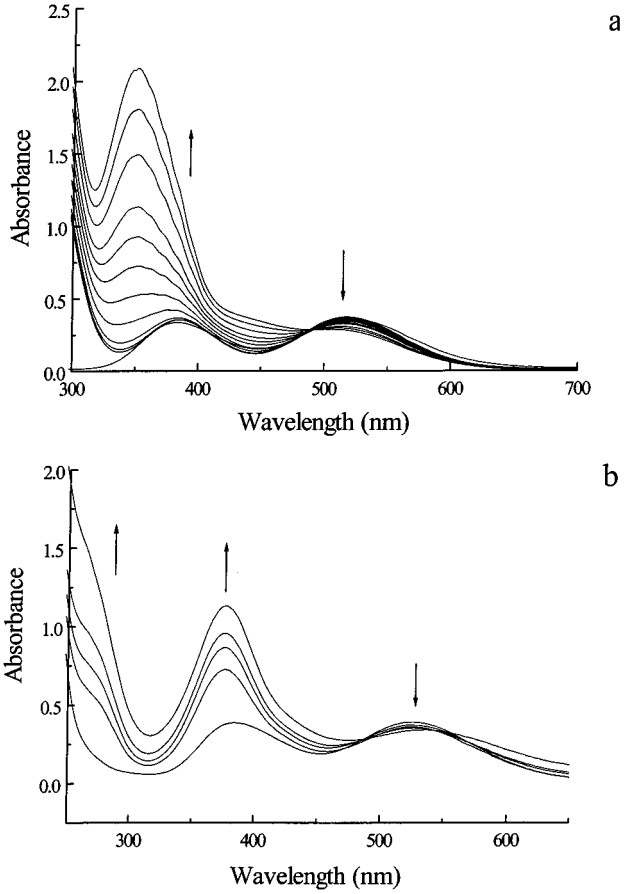

Figure 2. UV−vis spectral changes during the oxidation of $[Cr^{III}(Aib)_3]$ by (a) HIO_4 (one-molar equivalence, ~20 °C, at 0, 1, 5, 10, 20, 30, 40, 50, 60, 80, 100, and 120 min) and (b) PbO_2 (four-molar equivalence, 37 °C, at 0, 1, 5, 10, and 60 min).

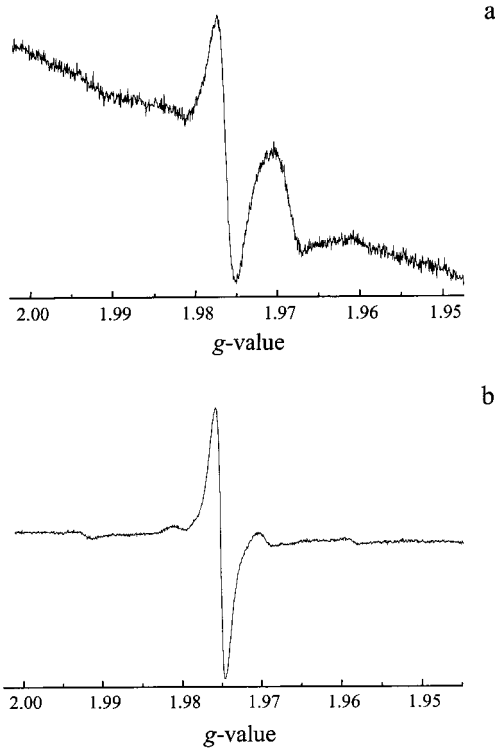

Figure 3. X-band EPR spectra of the Cr(V)−intermediates formed after reacting $Na_2Cr_2O_7{\cdot}2H_2O$ (50 mM) in methanol with (a) glycine (200 mM) for 15 d in the light and (b) alanine (200 mM) for 1 d in the dark.

The reaction of Cr(VI) and glycine in MeOH performed in the dark gave similar Cr(V) signals, but they were very weak compared with those resulting from the reaction in light. No color change was observed over the three-week period for dark reactions, hence, it was concluded that light was required for this reaction to proceed at an appreciable rate.

The Cr(VI)/MeOH reaction in the presence of alanine resulted in one Cr(V) EPR signal, which was observed in both light and dark reactions. Figure 3b shows the spectrum recorded for the reaction performed in the dark after day 1. The Cr(V) signal had a g_{iso} value of 1.9754 and a total line width of 4.88×10^{-4} cm^{-1}. Four satellite signals due to ^{53}Cr-hyperfine coupling were also observed with an A_{iso}(Cr) value of 17.89×10^{-4} cm^{-1}. The reaction was monitored over several days and while the g_{iso} value remained constant, the signal broadened; the total line width increased to 5.35×10^{-4} cm^{-1} by day 5 of the reaction. The reaction performed in the presence of light resulted in the same Cr(V) signal, but the reaction proceeded at a much faster rate and the signal intensity decreased and broadened rapidly over a 12-day period with the formation of a fine red-pink precipitate. In a reaction (in either the light or the dark) with excess Ala, the red-pink precipitate was isolated in high yield. Microanalysis and spectroscopic data showed that it was identical to $[Cr^{III}(Ala)_3]$ formed via Cr(III) synthesis methods. No EPR signals were observed from the brown solids isolated from the Cr(VI)/MeOH reductions in the presence of glycine and alanine or their solutions.

The reaction of Cr(VI) with Aib was similar to the alanine reaction in that Cr(V) EPR signals were detected for both dark and light reactions. However, the dark reaction yielded only very weak signals at $g_{iso} = 1.9765$ and 1.9806. When the reaction solution was exposed to light for 6 d, a very broad Cr(V) signal was observed and the second-derivative plot showed six superhyperfine lines (Figure 4a). The signal had a g_{iso} value of 2.0058 and the superhyperfine structure was much broader than any other signals. The total line width was 35.02×10^{-4} cm^{-1}, with $a_N = 13.3 \times 10^{-4}$ cm^{-1} and $a_H = 5.24 \times 10^{-4}$ cm^{-1}. When the reduction reaction was repeated using *N*-deuterated ligand in CH_3OD, the superhyperfine coupling simplified to a triplet (Figure 4b). This confirms that the superhyperfine coupling (Figure 4a) were due to a single nitrogen atom with one proton. When the reaction was performed with excess Aib ligand (again in either the light or the dark), $[Cr^{III}(Aib)_3]$ was isolated, which was analytically identical to that formed via the Cr(III) synthesis methods.

Positive-Ion ESMS. The positive-ion ESMS for the glycine complex had a peak at $m/z = 297$ corresponding to the 2+ ion, $[Cr_2O_4(C_2H_4NO_2)(OH_2)_3]^{2+}$, which would be a mixed-valence Cr(V)/Cr(VI) ion. There was also a peak at $m/z = 413$ corresponding to $\{[Cr_2O_4(C_2H_4NO_2)_2(CH_3O)_2]^{2-} + 3H^+ + CH_3OH\}^+$ indicating a similar structure to the alanine dimer. The parent ion is also observed in the peak at 457 corresponding to $\{[Cr_2O_4(C_2H_4NO_2)_2(CH_3O)_2]^{2-} + H^+ + 2Na^+ + CH_3OH\}^+$.

The positive-ion ESMS of the Cr(V)−Ala complex exhibited a fragment at $m/z = 206$ corresponding to $\{[Cr(O)_2(C_3H_6NO_2)\text{-}(CH_3O)]^- + 2H^+\}^+$, a dimeric fragment in which one of the alanine ligands had been lost at $m/z = 356$ corresponding to $\{[Cr_2O_4(C_3H_6NO_2)(CH_3O)_2(H_2O)_2]^- + 2H^+\}^+$ and a peak containing the parent complex at $m/z = 450$ corresponding to $\{[Cr_2O_4(C_3H_6NO_2)_2(CH_3O)_2]^{2-} + Na^+ + 2H^+ + H_2O\}^+$.

XANES. The X-ray absorption near-edge structure of $[Cr^{III}(Aib)_3]$ and $Na_2[Cr^{V}_2O_4(Ala)_2(OCH_3)_2].0{\cdot}5(AlaH).0{\cdot}5CH_3OH$ are given in Figure 5. The height of the $\{[Cr^{V}O(Ala)(OCH_3)\text{-}$

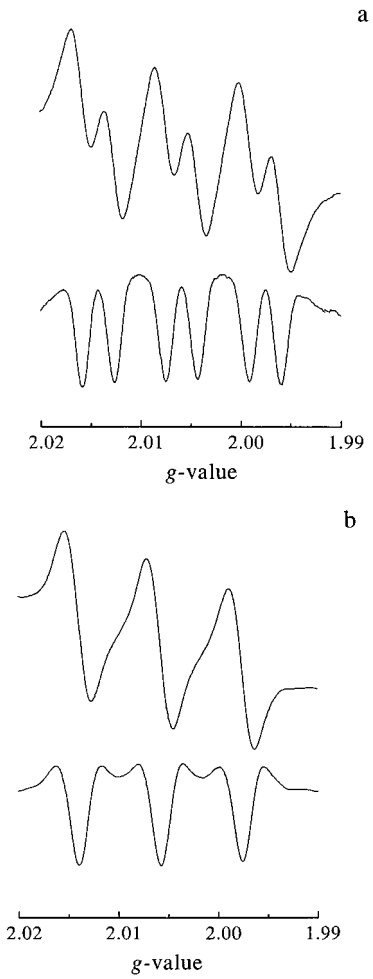

Figure 4. X-band EPR spectra and second-derivative spectra of the Cr(V) complex formed after reacting $Na_2Cr_2O_7 \cdot 2H_2O$ (50 mM) with: (a) Aib (200 mM) in methanol; and (b) deuterated Aib (200 mM) in deuterated methanol; both in the presence of light and after 6 d of reaction.

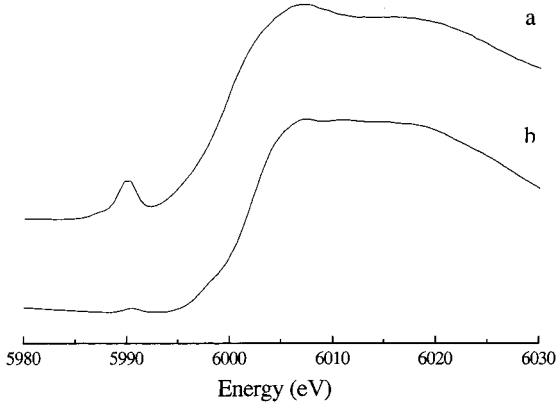

Figure 5. XANES in BN matrixes obtained from: (a) $Na_2[Cr^{V}_2O_4(Ala)_2(OCH_3)_2].0 \cdot 5(AlaH).0 \cdot 5CH_3OH$; and (b) $[Cr^{III}(Aib)_3]$.

$(\mu\text{-O})]_2\}^{2-}$ preedge peak (Figure 5a) is ~18% of the height of the most intense edge peak, which is typical of the moderate-intensity Cr(V) 1s → 3d transitions, although somewhat less intense than those of five-coordinate mononuclear complexes.[39−41] The height of the $[Cr^{III}(Aib)_3]$ preedge peak (Figure 5b), at ~2.5% of the edge height, is typical of Cr(III).[39−41]

(39) Ellis, P. J.; Joyner, R. W.; Maschmeyer, T.; Masters, A. F.; Niles, D. A.; Smith, A. K. *J. Mol. Catal. A. Chem.* **1996**, *111*, 297−305.

Table 3. Goodness-of-Fit Parameters for Refined Models II−VII

model	R	R_{XAFS}	determinacy
II	15.38%	13.32%	1.11
III	20.43%	17.57%	1.26
IV	14.24%	12.24%	1.21
V	16.30%	14.40%	1.18
VI	21.56%	20.69%	1.37
VII	18.65%	14.90%	1.18

XAFS Structure of Cr(V)−Alanine Complex. The lack of a Cr(V) EPR signal from the solid product, and the presence of dinuclear ions in the ES/MS spectrum indicated that it was a dimer. The EPR spectrum of the mononuclear Cr(V) intermediate was assigned to a six-coordinate species, so **II**, **IV**, **V**, and **VII** were used as models in XAFS fits**.** Mononuclear, **III,** and five-coordinate, **VI**, models were also examined. Initially, fits to the XAFS data with model **II** were carried out with R_{max} of 6.50 Å, but there was no significant backscattering of the photoelectron from the carbon backbone of the more distant alanine. The low contributions to the XAFS from these atoms are due to the fact that usually only scattering from atoms within 4−5 Å of the absorber affects the XAFS.[28−30] The only significant contributions to the XAFS from the distant alanine ligand were due to the O and N atoms coordinated to the second Cr, so the remaining atoms were removed from **II** to give model **IV**. As a result, the R_{max} value was decreased to 5.50 Å, and this value was used in fits to models **II**−**VII**.

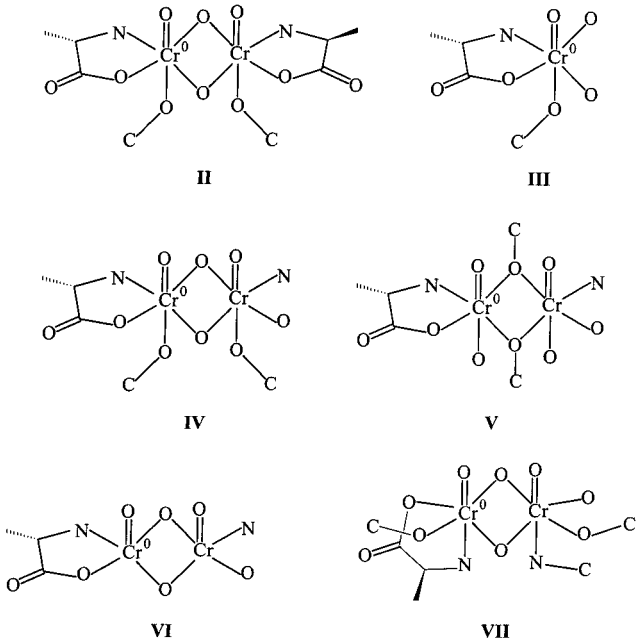

Mononuclear and dinuclear models with both five- and six-coordinate Cr atoms were compared in preliminary refinements. The XAFS calculated for six-coordinate dinuclear models gave the best fits to the observed XAFS (Table 3). The best fit to the observed XAFS was obtained with **IV** (restraints and constraints are included in the Supporting Information, Tables S11 and S12). Model **IV** gave a slightly better fit than model **II** because the restraints for the extra shells of **II** are included in the goodness-of-fit parameters, but the extra shells made no significant contributions to the XAFS. The mononuclear model

(40) Levina, A.; Foran, G. J.; Lay, P. A. *J. Chem. Soc., Chem. Commun.* **1999**, *23*, 2339−2340.
(41) Codd, R.; Levina, A.; Zhang, L.; Hambley, T. W.; Lay, P. A. *Inorg. Chem.* **2000**, *39*, 990−997.

Table 4. Selected Bond Lengths, Interatomic Distances and Bond Angles from the Refinement of **IV** Using the XAFS Data[a]

bond lengths or interatomic distances (Å)		bond angles (deg)	
Cr0−O1	1.96(2)	O1−Cr0−O4	168(5)
Cr0−N2	2.03(2)	N2−Cr0−O3	167(5)
Cr0−O3	1.94(2)	O3−Cr0−O4	78(1)
Cr0−O4	1.94(2)	O5−Cr0−O10	166(4)
Cr0−O5	1.56(2)	O3−Cr12−O4	78(1)
Cr0−O10	1.74(2)	Cr0−O3−Cr12	99(1)
O10−C11	1.36(2)	Cr0−O4−Cr12	99(1)
Cr0−Cr1	2.95(2)		
O3−O4	2.45(2)		

[a] The estimated error in the last significant figure is shown in parentheses. The errors in the bond lengths and interatomic distances are the root-mean-square (rms) combination of the conservative systematic error[28−30] with the error determined by Monte Carlo analyses.[19,20] The errors in the bond angles are the rms combination of the Monte Carlo error and the error in the bond angle due to the Monte Carlo error in the bond lengths.[31]

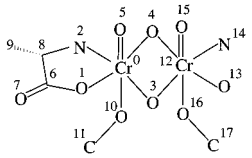

Figure 6. Diagram of model **IV** showing the atom-numbering scheme.

III resulted in a much poorer fit to the observed XAFS. The higher values of R for **III** as opposed to **IV** indicated that the complex was dinuclear, which was confirmed by the presence of significant MS pathways involving the second Cr atom in the refined model **IV** (Supporting Information, Table S13).

Model **V** (a truncated model like **IV**) is just as consistent with the electrospray mass spectrometry and microanalytical data as **IV**, but it gave a significantly worse fit to the observed XAFS. This indicated that the methoxo ligands are unlikely to act as bridging ligands, but are coordinated trans to the oxo groups. The truncated five-coordinate model, **VI**, had significantly higher R_{XAFS} value than **IV**, which indicated that the Cr was six coordinate. The coordination of the alanine with the amine trans to the oxo group and cis to the two bridging oxygen atoms was examined in model **VII**. The value of R_{XAFS} was significantly increased, so both the amine and carboxylate groups of alanine are likely to be coordinated cis to the oxo and methoxo groups.

Other possible isomers of **II** are difficult to distinguish by XAFS. The two oxo groups can be syn or anti; the syn isomer had somewhat lower goodness-of-fit values, but there is little difference between the XAFS fits to the two models. In **II,** the alanine ligands were arbitrarily arranged in a cis geometry, but when they were trans, the R_{XAFS} value increased. Distinguishing between N and O atoms by XAFS is very difficult, and often impossible because their backscattering amplitudes and phases are similar,[28,30] so a distinction relies on small differences in MS pathways involving the noncoordinating atoms of the trans and cis isomers. The bond distances to the O and N atoms of the alanine ligand coordinated to Cr could be accurately distinguished because there were strong MS paths involving the C atom and the two O atoms of the carboxylate group from the alanine ligand (Table S13). Selected bond lengths, interatomic distances and bond angles for **IV** are contained in Table 4 and the atom-numbering scheme is given in Figure 6. The observed XAFS and Fourier transform curves are shown in Figures 7a and 7b, respectively, along with the curves calculated for **IV** and the window functions.

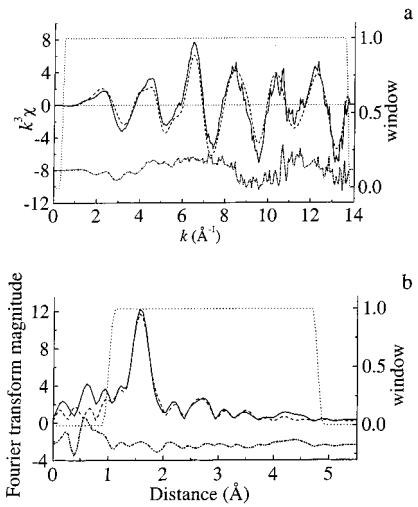

Figure 7. (a) XAFS and (b) Fourier transform amplitude of XAFS for $Na_2[Cr^V_2O_4(Ala)_2(OCH_3)_2].0{\cdot}5(AlaH).0{\cdot}5CH_3OH$: observed (solid line), calculated from refined model **IV** (dashed line), residual (dot−dash line) along with the window used (dotted line).

BVS Calculations. The BVS analysis of **II** gave a value of 4.74 for the Cr oxidation state, which was in good agreement with the expected value of 5. In a previous BVS analysis of Cr complexes with O donor ligands, values within 0.30 of the integer value were considered to be acceptable.[37] It was also noted that the use of an average value for R_0 tended to result in an underestimation of the BVS for Cr(V) complexes. The BVS analysis confirmed the interpretation of the XANES spectrum and showed that the Cr−ligand bond lengths determined by XAFS were reasonable.

Discussion

Reduction of Cr(VI) in the Presence of Amino Acids. Initial attempts to prepare Cr(V) amino acid complexes by the reduction of Cr(VI) using the method of Krumpolc and Roček[42−44] were unsuccessful. This method required stirring a solution containing Cr(VI) and the appropriate ligand in acetone for ∼24 h in the dark. It was straightforward for Cr(V)/tertiary hydroxy acid complexes, because the ligands were soluble in acetone and they reduced Cr(VI) to Cr(V). EPR spectroscopic studies of the Cr(VI)/MeOH reaction in the presence of peptides showed that Cr(V)−peptide complexes were formed, with MeOH acting as the solvent and reductant.[13] The reduction of Cr(VI) with Gly, Ala, and Aib showed that both Cr(V) and Cr(III) complexes were formed. In the presence of excess ligand, the reactions with Ala and Aib resulted in the formation of Cr(III) complexes. Light was required to speed up the reaction, except for the alanine complex, which was also formed in the dark. Although the reaction solutions showed weak monomeric Cr(V) EPR signals, EPR-silent complexes were isolated, consistent with the formation of Cr(V) dimers.

The shifts in λ_{max} values in the electronic absorption spectra were also consistent with the formation of Cr(V) complexes from Cr(VI). The MeOH solution spectrum of $Na_2Cr_2O_7$ has peaks at 212, 258 and 352 nm, with a shoulder at 434 nm. For

(42) Krumpolc, M.; DeBoer, B. G.; Roček, J. *J. Am. Chem. Soc.* **1978**, *100*, 145−153.
(43) Judd, R. J.; Hambley, T. W.; Lay, P. A. *J. Chem. Soc., Dalton Trans.* **1989**, 2205−2210.
(44) Krumpolc, M.; Roček, J. *J. Am. Chem. Soc.* **1979**, *101*, 3206−3209.

the Cr(V) dimers of glycine and alanine, there was a major peak at 380 and 374 nm, respectively, with $\epsilon_{max} \sim 1400\ M^{-1}\ cm^{-1}$. Solid products isolated from the reaction of Cr(VI) with Aib had a λ_{max} at 376 nm; and a ϵ_{max} value of 2440 $M^{-1}\ cm^{-1}$, which suggests the presence of unreacted Cr(VI). Also, the EPR spectra attained from the Cr-Aib reaction solution had a sloping background, which indicated the presence of Cr(III) species. The ES/MS of the Cr(V)−Ala complex confirmed the presence of both the dimer and monomeric fragmentation species, which were consistent with the given formula. The ES/MS of the Cr(V)−Gly complex also produced peaks consistent with a dimeric species and it is likely to have a similar structure as the alanine complex.

Oxidation of Chromium(III) Complexes. Oxidation of $[Cr(Aib)_3]$ using either PbO_2 or HIO_4, revealed no Cr(V) EPR signals, but the solution changed from pink to yellow with concomitant growth of UV−vis peaks indicative of Cr(VI). The UV−vis spectra of the HIO_4 oxidation products were similar to those obtained for the periodate oxidation of $[Cr(Val)_2(H_2O)_2]^+$ (Val = *DL*-valine).[45] Periodate readily oxidizes both inert and labile complexes and IO_4^- is thought to be capable of acting as a ligand.[46,47] Kinetic studies involving oxidation of the latter complex in aqueous medium led to the suggestion of an inner-sphere mechanism, which was believed to proceed via a one- or two-electron-transfer process giving Cr(IV) or Cr(V) intermediates, respectively.[48] The Cr(III) amino acid complexes are less easily oxidized than the peptide complexes and the latter appear to form Cr(V) products more readily.[11−13]

Characterization of Cr(V)−Amino Acid Intermediates. The Cr(VI)/MeOH reduction in the presence of amino acids produced a number of EPR signals due to monomeric Cr(V) complexes. The Cr(V)−Ala complex with a signal at $g_{iso} = 1.9754$ is assigned as a six-coordinate species, **VIII** (or a geometric isomer), which has a calculated *g* value of 1.9754, based on empirical parameters.[11−13,49] This species could be either an intermediate en route to the formation of the EPR-silent dimer, or is in equilibrium with the dimer. Since dissolution of the dimer in water does not produce an EPR signal, it is unlikely that the two species are in equilibrium.

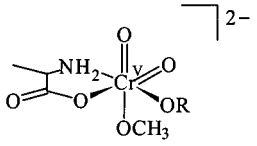

R = H, CH_3

VIII

The Cr(VI)/MeOH reaction in the presence of Gly produced Cr(V) signals that were similar to those observed in the absence of Gly and were assigned to Cr(V)/methoxo species. The signal at 1.9765 is consistent with the six-coordinate Cr(V)−oxo species **IX,** and the signal at 1.9687 is most probably a Cr(V)−Cr(VI) dimer.[11,12] The Cr(V)−glycine product was isolated from the reaction solution as a brown precipitate and was EPR silent, both in the solid state and in aqueous solution. However, the complex gave a similar electronic absorption spectra to the Cr(V)−alanine dimer complex and thus was tentatively characterized as having a similar structure as the Cr(V)−alanine dimer.

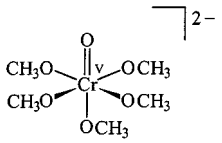

IX

The reduction of Cr(VI) with Aib produced different results. A monomeric Cr(V) complex being formed, which had a relatively high *g* value compared with the other Cr(V)−peptide and amino acid complexes. Its EPR spectrum, together with the results of the deuteration experiments, show the presence of one Aib ligand that was deprotonated at the nitrogen; consistent with structure **X**. The high g_{iso} value (2.0058) is indicative of a five-coordinate species.[49] The high a_N and a_H values, combined with the value typical for an organic radical, is indicative of considerable delocalization of the electron onto the ligand. The product isolated from the reaction solution was EPR-silent but was likely to be a mixture of Cr(VI), Cr(V) and Cr(III) species. Indeed, the EPR spectra of the reaction solution had a distinctive slope suggesting the presence of Cr(III), while the UV−vis spectra suggested the presence of unreacted Cr(VI). The difference among the amino acids most likely resides in the fact that species such as **X** would result in rapid oxidative dehydrogenation reactions to form imines according to eq 3. Such reactions are not possible with the Aib complex.

$$Cr^{V}–\bar{N}H–CHR \rightarrow Cr^{III}–NH=CR + H^+ \qquad (3)$$

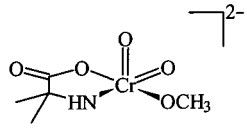

X

Characterization of the Cr(V)−Alanine Dimer. The few reports of isolated and structurally characterized dinuclear Cr(V) complexes include crystal structures for an azide-bridged,[50] a bis(μ-imido),[51] and two bis(μ-oxo)[52,53] dinuclear Cr(V) complexes. The average Cr−(μ-O) bond length in $Li_2\{[Cr^{V}O(PFP)(\mu\text{-}O)]_2\}\cdot 2H_2O.2py$[52] (PFP = perfluoropinacolate(2-), py = pyridine) was 1.812 Å. The average Cr−(μ-O) bond length in $\{[Cr^{V}O(CpMe_5)(\mu\text{-}O)]_2\}$[53] (where $CpMe_5$ is the pentamethylcyclopentadienyl ligand) was 1.815 Å. The Cr−(μ-O) bond lengths in **II** are approximately 0.13 Å longer than the Cr−(μ-O) bond lengths in these complexes. This large increase in the Cr−(μ-O) bond lengths in **II** could be attributed to a couple of factors. The Cr atoms in **II** are six-coordinate while in $Li_2\{[CrO(PFP)(\mu\text{-}O)]_2\}\cdot 2H_2O.2py$ each Cr atom was five-coordinate and was coordinated to two μ-oxo ligands, an oxo group and the bidentate PFP^{2-} in a square-pyramidal environment, and in $\{[Cr^{V}O(CpMe_5)(\mu\text{-}O)]_2\}$ each Cr atom was coordinated to two μ-oxo ligands, an oxo group and a $CpMe_5$ ligand in a distorted

(45) Abdel-Khalek, A. A.; Sayyah, E. M.; Ewais, H. A. *Transition Met. Chem.* **1997**, *22*, 375−380.
(46) Hadinec, I.; Jensovsky, L.; Linek, A.; Synecek, V. *Naturwiss* **1960**, *47*, 377.
(47) Ray, P. *Inorg. Synth.* **1957**, *5*, 201−204.
(48) El-Eziri, F. R.; Sulfab, Y. *Inorg. Chim. Acta* **1977**, *25*, 15−20.
(49) Barr-David, G.; Charara, M.; Codd, R.; Farrell, R. P.; Irwin, J. A.; Lay, P. A.; Bramley, R.; Brumby, S.; Ji, J.-Y.; Hanson, G. R. *J. Chem. Soc., Faraday Trans.* **1995**, *91*, 1207−1216.
(50) Meyer, K.; Bendix, J.; Bill, E.; Weyhermueller, T.; Wieghardt, K. *Inorg. Chem.* **1998**, *37*, 5180−5188.
(51) Danopoulos, A. A.; Wilkinson, G.; Sweet, T. K. N.; Hursthouse, M. B *J. Chem. Soc., Dalton Trans.* **1995**, 2111−2123.
(52) Nishino, H.; Kochi, J. K. *Inorg. Chim. Acta* **1990**, *174*, 93−102.
(53) Herberhold, M.; Kremnitz, W.; Razavi, A.; Schöllhorn, H.; Thewalt, U. *Angew. Chem., Int. Ed. Engl.* **1985**, *24*, 601−602.

tetrahedral environment. The higher coordination number for the Cr atoms in **II** may lead to a weaker interaction with the μ-O groups and longer bond lengths. The other explanation is that the Cr atoms in **II** are coordinated by two short, strong bonds to the terminal oxo group and the methoxo oxygen; this would lead to a lengthening of the Cr−(μ-O) bond lengths. Since hydrogen atoms are not normally significant contributors to the XAFS, it is possible that the two bridging ligands in **II** are hydroxo groups rather than oxo groups. This would require that the complex is a dinuclear Cr(IV) species rather than a Cr(V) species, which is inconsistent with the valence-bond calculations.

The 1.74(2) Å Cr−O(methoxo) distance in **II** is similar to, but a shorter than, the Cr−O(alkoxo) distances of 1.767−1.798 Å in $Na[Cr^{V}O(ehba(2-))_2]\cdot 1.5H_2O$[43] and $K[Cr^{V}O(hmba(2-))_2].H_2O$.[44] This is unusual, especially considering the strong trans influence of the oxo ligand. The short Cr−O(methoxo) bond appears to be real because the Cr−O or Cr−N bond lengths trans to the oxo group were in the range 1.72−1.74 Å in all fitted models. Short M−O(methoxo) bonds have been reported in crystal structures of V(V) complexes, i.e., 1.723 Å,[54] 1.760 and 1.783 Å.[55] The Cr−O(oxo) length of 1.56(2) Å is typical of Cr(V), and the Cr−O(carboxylato) bond length of 1.96(2) Å is slightly longer than the values of 1.90−1.92 Å reported in crystal structures.[42,43,52,53]

The close match between the experimental and observed curves in the 2−4 Å region of the Fourier transform indicates that MS scattering analysis can accurately determine structural details for the dimer. The results of the XAFS analysis of $Na_2[Cr^{V}_2O_4(Ala)_2(OCH_3)_2].0\cdot 5(AlaH).0\cdot 5CH_3OH$ provided strong evidence that structure **II** (of which the best model, **IV**, was a truncated version) is correct.

(54) Dutta, S. K.; Kumar, S. B.; Bhattacharyya, S.; Tiekink, E. R. T.; Chaudhury, M. *Inorg. Chem.* **1997**, *36*, 4954−4960.
(55) Jiang, F.; Anderson, O. P.; Miller, S. M.; Chen, J.; Mahroof-Tahir, M.; Crans, D. C. *Inorg. Chem.* **1998**, *37*, 5439−5451.

Conclusion

In conclusion, the first Cr(V) complexes were characterized with biologically relevant non-sulfur-containing amino acids. Chromium(V) amino acid complexes are formed during the reduction of Cr(VI), although the ligands did not actually reduce Cr(VI). These reactions occurred in the presence and absence of light and the end products of reactions performed in excess were Cr(III) amino acid complexes. However, reactions involving glycine required light for the reaction to proceed.

Acknowledgment. We thank the Australian Research Council (Large Grant P.A.L.; and RIEFP grants for the EPR spectrometers, ESMS equipment, X-ray diffractometer, and 10-element Ge detector) for support. X-ray absorption spectroscopy was performed at the Australian National Beamline Facility (ANBF) with support from the Australian Synchrotron Research Program, which is funded by the Commonwealth of Australia under the Major National Research Facilities program. H.A.H. and C.L.W. are grateful for funding through Worksafe Australia and Australian Postgraduate Awards, respectively. We would like to thank Drs. Garry Foran and James Hester of the Australian National Beamline Facility, and Dr. Aviva Levina for assistance in recording the XAS data, and Dr. Nicholas Dixon from the Australian National University for microanalyses and helpful discussions.

Supporting Information Available: Table S1−S9, tables of non-hydrogen atom and hydrogen coordinates, anisotropic thermal parameters for the non-hydrogen atoms, non-hydrogen bond lengths and angles, torsion angles, hydrogen-bond geometries and bond lengths, and angles involving hydrogen atoms for *fac*-$[Cr(Aib)_3]$; Table S10, electronic absorption data for Cr(III) and Cr(V) amino acid complexes; and Tables S11-S14, details of restraints, constraints, multiple-scattering paths, and Debye−Waller factors, respectively, in the refinement of **IV**. This material is available free of charge via the Internet at http://pubs.acs.org.

IC010377L